

Fig. 3.4 Energy levels of the Ne atom which can be interpreted as the promotion of a $2p$ electron to the available empty orbitals starting with $3s$ etc. Also for this atom the energies of the states tend to become more Hydrogen-like with increasing “ n ” and l .

action of the Coulomb interaction depending on which total angular momentum the resulting configuration has.

3.3 Nucleons in nuclei

The shell structure observed in atoms is also found in nuclei. The origin of shell structure in nuclei is, however, quite different. In addition, it is not as simple to understand as in the atomic case. The shell structure in atoms can be demonstrated by considering the ionization energy as in Fig. 3.1. Shell closures at 2, 10, 18, 36, 54, and 86 which signal the position of the noble gas atoms, are then clearly visible. In the case of nuclei a similar quantity, called separation energy, should be considered. For neutrons it is

defined by

$$S_n(N, Z) = B(N, Z) - B(N - 1, Z) \quad (3.17)$$

and for protons by

$$S_p(N, Z) = B(N, Z) - B(N, Z - 1), \quad (3.18)$$

where B describes the nuclear binding energy for the nucleus as a function of N , the number of neutrons, and Z , the number of protons and is defined by considering the total mass of the nucleus

$$\begin{aligned} M(N, Z) &= E(N, Z)/c^2 \\ &= N m_n + Z m_p - B(N, Z)/c^2. \end{aligned} \quad (3.19)$$

By considering the separation energy shell closures become visible as shown for $N = 126$ in Fig. 3.5. A shell closure appears for fixed values of the difference $N - Z$ as a function of N but does display an odd-even staggering that can be interpreted in terms of additional stability of systems with even number of neutrons. One can eliminate this staggering by considering the separation energy only for odd N with Z even, as a function of the number of neutrons as has been done in Fig. 3.5 or, for protons, for Z odd and N even. Such considerations then identify shell closures at $N = 50, 82,$ and 126 and at $Z = 50$ and 82 . Less clear, but deduced from other data, like spectra and magnetic moments, are shell closures for both N and Z corresponding to 2, 8, 20, and 28 [Bohr and Mottelson (1998)]. Historically, it was more difficult to relate these “magic” numbers to shell closures than in the atomic case.

The sp potential that is responsible for this type of shell structure is generated by the nucleons themselves since there is no center of attraction as in the case of electrons. Ultimately such a sp potential must be related to the interactions between the nucleons which are responsible for the binding of the system. For now, it is useful to consider an empirical sp potential which provides an adequate description of nuclear shell structure and is given by [Bohr and Mottelson (1998)]

$$U = V f(r) + V_{\ell s} \left(\frac{\boldsymbol{\ell} \cdot \mathbf{s}}{\hbar^2} \right) r_0^2 \frac{1}{r} \frac{d}{dr} f(r) \quad (3.20)$$

with

$$f(r) = \left[1 + \exp \left(\frac{r - R}{a} \right) \right]^{-1}. \quad (3.21)$$

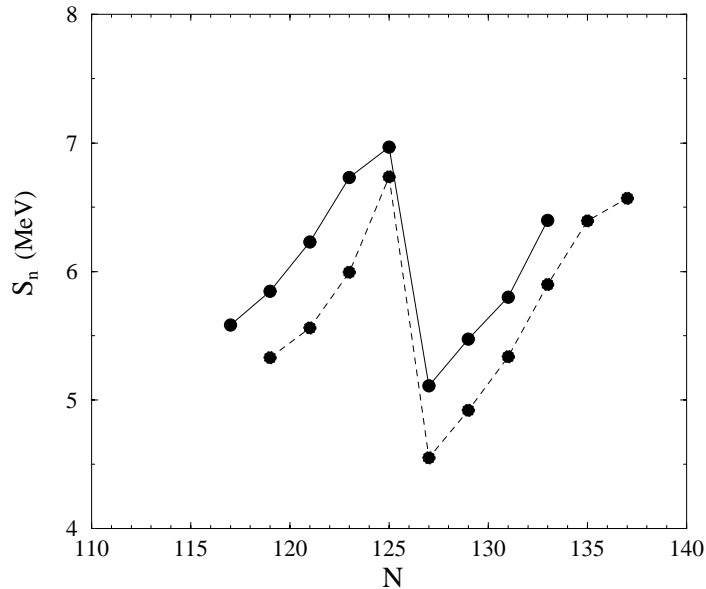


Fig. 3.5 Neutron separation energies for nuclei in the Pb region. Only even Z nuclei are used in this plot. The full line corresponds to $N - Z = 41$, the dashed line to $N - Z = 43$.

This form is referred to as a Woods-Saxon shape. The depth of this potential is given by

$$V = \left[-51 \pm 33 \left(\frac{N - Z}{A} \right) \right] \text{ MeV}, \quad (3.22)$$

where the plus sign is for neutrons and the minus sign for protons. The radius parameter is given by

$$R = r_0 A^{1/3}, \quad (3.23)$$

with $r_0 = 1.27$ fm, the diffuseness parameter $a = 0.67$ fm, and the strength of the spin-orbit interaction $V_{\ell s} = -0.44V$. For protons one also has to consider their mutual Coulomb repulsion which can be reasonably represented by the potential of a homogeneous sphere with charge $Z - 1$ and radius $R_C = R$. A parametrization of this kind is successful in describing some of the properties of the lowest energy states of nuclei with one more or less proton or neutron with respect to the ground-state energy of doubly magic nuclei like ^{208}Pb . A comparison with experimental data is shown in Fig 3.6. In the independent-particle model, the ground state of this nucleus

is obtained by filling the relevant proton and neutron shells. The lowest-energy states for the $A = 209$ system are obtained by adding a proton or neutron in the corresponding lowest available empty shells. The observed and calculated positions of these levels show a good correspondence which is also observed for odd nuclei neighboring other nuclei like ^{16}O , ^{40}Ca , ^{48}Ca , and ^{56}Ni which also have closed shells for both protons and neutrons. The energy of an additional proton or neutron for an $A = 209$ system in this simple model is given by

$$\hat{H}_0 a_\alpha^\dagger |^{208}\text{Pb}_{g.s.}\rangle = [\varepsilon_\alpha + E(^{208}\text{Pb}_{g.s.})] a_\alpha^\dagger |^{208}\text{Pb}_{g.s.}\rangle \quad (3.24)$$

where α represents the quantum numbers of an unoccupied proton or neutron state. The experimental information is obtained by subtracting from the ground-state energy of ^{209}Bi or ^{209}Pb the ground-state energy of ^{208}Pb , which gives the position of the first “empty” level for an extra proton or neutron, respectively. The position of the other experimental levels can then be obtained by adding their excitation energy to the sp energy corresponding to the ground state of the appropriate $A = 209$ system. One should observe that this procedure allows a comparison with the sp levels obtained from the Woods-Saxon potential although the comparison presupposes that the independent-particle model is appropriate. For the states in the $A = 207$ systems one has in the independent-particle description

$$\hat{H}_0 a_\alpha |^{208}\text{Pb}_{g.s.}\rangle = [E(^{208}\text{Pb}_{g.s.}) - \varepsilon_\alpha] a_\alpha |^{208}\text{Pb}_{g.s.}\rangle. \quad (3.25)$$

The calculated position of the levels again corresponds to ε_α and can be compared with experiment for the last occupied “sp” state by subtracting the ground-state energy of the relevant $A = 207$ system from $E^{(0)}(^{208}\text{Pb})$. Higher excited states in these systems therefore occur lower in energy (are more deeply bound) in this picture as shown in Fig 3.6. The position of the sp levels compares favorably with the experimental data although there are clearly some details missing.

A Woods-Saxon potential has a finite depth and therefore has a finite number of bound states contrary to a Hydrogen-like potential which has an infinite number of bound states. It also has an exponential fall-off at large r which implies that all bound states are well localized, again contrary to the r^{-1} behavior of a Hydrogen-like potential with the resulting large mean-square radii of weakly bound orbitals. The central part of the Woods-Saxon

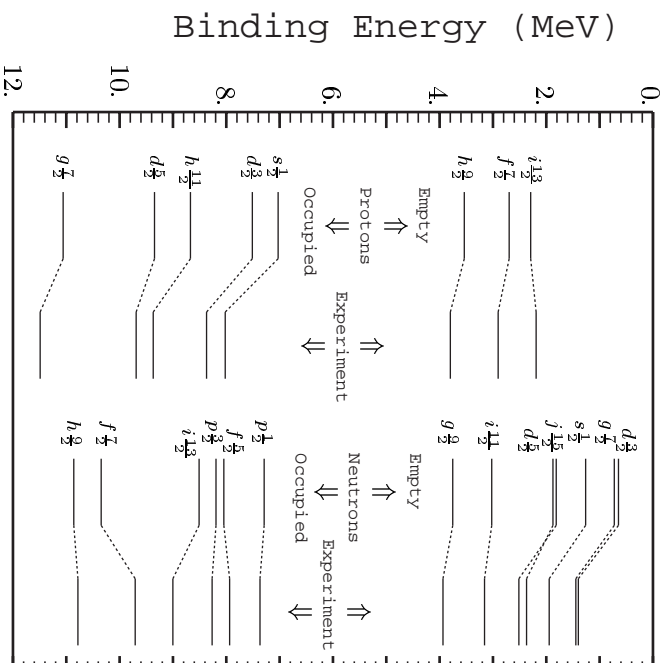


Fig. 3.6 Energy levels of particles and holes with respect to ^{208}Pb . The results for the empirical potential are shown in the first column for protons and the third column for neutrons. These levels are compared with the corresponding experimental data for protons in the second and for neutrons in the fourth column.

potential can be reasonably approximated by a three-dimensional harmonic oscillator (HO) potential

$$U_{HO}(r) = \frac{1}{2}m\omega^2 r^2 - V_0. \quad (3.26)$$

The oscillator frequency ω and constant shift V_0 can be adjusted to resemble the Woods-Saxon well as shown in Fig. 3.7. The HO potential has only discrete eigenstates and care needs to be exercised to interpret the positive energy states which correspond to scattering states for the Woods-Saxon well. The eigenvalues of the HO potential are given by

$$H_{HO} |n\ell m_s\rangle = (h\omega(2n + \ell + \frac{3}{2}) - V_0) |n\ell m_s\rangle \quad (3.27)$$

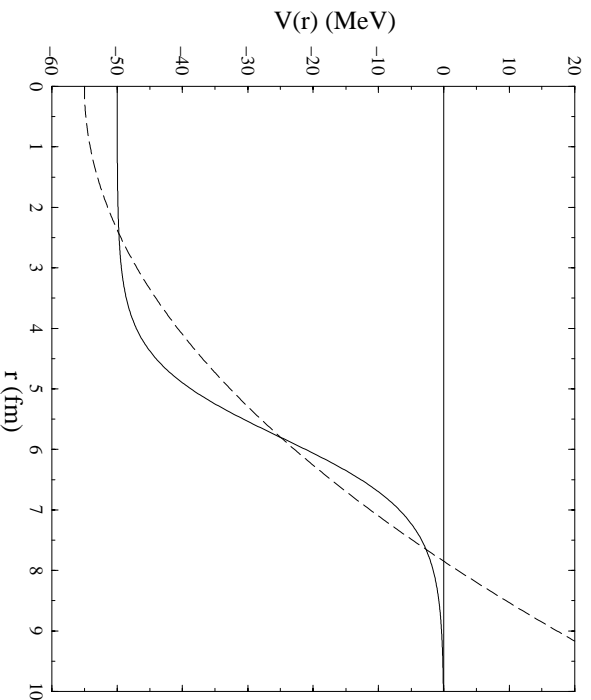


Fig. 3.7 Comparison of the central part of the Woods-Saxon potential given in Eq. (3.20) with an adjusted HO potential for $A = 100$.

with

$$\begin{aligned} n &= 0, 1, 2, \dots \\ \ell &= 0, 1, 2, \dots \\ -\ell &< m_\ell < \ell. \end{aligned} \tag{3.28}$$

The total number of oscillator quanta is given by

$$N = 2n + \ell, \tag{3.29}$$

which implies according to Eq. (3.27) that for each oscillator energy only states with the same parity are degenerate. The HO potential by itself leads to magic numbers corresponding to 2, 8, 20, 40, 70, 112, and 168 as can be easily verified. Although the first three shell closures correspond to experimental observations, the others show little resemblance to experiment.

A Nobel prize winning suggestion was made by Goeppert-Mayer and Jensen in 1949 [Goeppert-Mayer (1949); Jensen *et al.* (1949)] who introduced, independently, a strong one-body spin-orbit potential similar to the

one given in Eq. (3.20). The effect of this potential is mostly felt at the surface of the nucleus since this is where the derivative of $f(r)$ (see Eq. (3.21)) peaks. The presence of the $\ell \cdot \mathbf{s}$ operator requires a change of sp basis to states with good total angular momentum

$$|n(\ell s)jm_j\rangle = \sum_{m_\ell m_s} |n\ell m_\ell m_s\rangle \langle \ell m_\ell s m_s | j m_j \rangle. \quad (3.30)$$

The transformation bracket is usually referred to as a Clebsch-Gordan coefficient [Sakurai (1994)]. Using the operator identity

$$\ell \cdot \mathbf{s} = \frac{1}{2}(\mathbf{j}^2 - \ell^2 - \mathbf{s}^2) \quad (3.31)$$

one finds

$$\frac{\ell \cdot \mathbf{s}}{\hbar^2} |n(\ell s)jm_j\rangle = \frac{1}{2}(j(j+1) - \ell(\ell+1) - \frac{1}{2}(\frac{1}{2}+1)) |n(\ell s)jm_j\rangle. \quad (3.32)$$

Obviously for an s -wave the spin-orbit potential does not contribute. For other ℓ -values one obtains for $j = \ell + \frac{1}{2}$ the eigenvalue $\frac{1}{2}\ell$ whereas for $j = \ell - \frac{1}{2}$ one has $-\frac{1}{2}(\ell+1)$ from Eq. (3.32). Combining this result with the sign of $V_{\ell s}$ and the sign of the derivative of $f(r)$ one deduces that the introduction of this spin-orbit interaction has the tendency to substantially lower the energy in a given major shell of the subshell with the largest orbital angular momentum and $j = \ell + \frac{1}{2}$. This behavior is confirmed by experiment in light nuclei but the shifts are not so large as to alter the main shell closures at 2, 8, and 20. The first deviation occurs for the $0f_{7/2}$ shell which becomes a major shell of its own leading to the observed shell closure at 28. In higher shells the lowering of this $\ell_{max} + \frac{1}{2}$ orbit is sufficiently large so that it comes to reside among the orbitals of the $N - 1$ major shell that have a different parity. This occurs for the $0g_{9/2}$ shell, leading to the shell closure at 50, the $0h_{11/2}$ with a resulting closure at 82, and finally with the $0i_{13/2}$ so that 126 also represents shell closure. These features are schematically indicated in Fig. 3.8, where the first column indicates the energy quantum number (not to scale) of the major shells of the HO together with their parity. The corresponding quantum numbers are given in the next column. Additional splitting of the HO degeneracy with the more realistic Woods-Saxon well, will also favor the higher ℓ orbitals. This feature together with the aforementioned spin-orbit effects are incorporated in the schematic splitting of the sp levels shown with appropriate sp quantum numbers are given together with the number of nucleons they can contain.

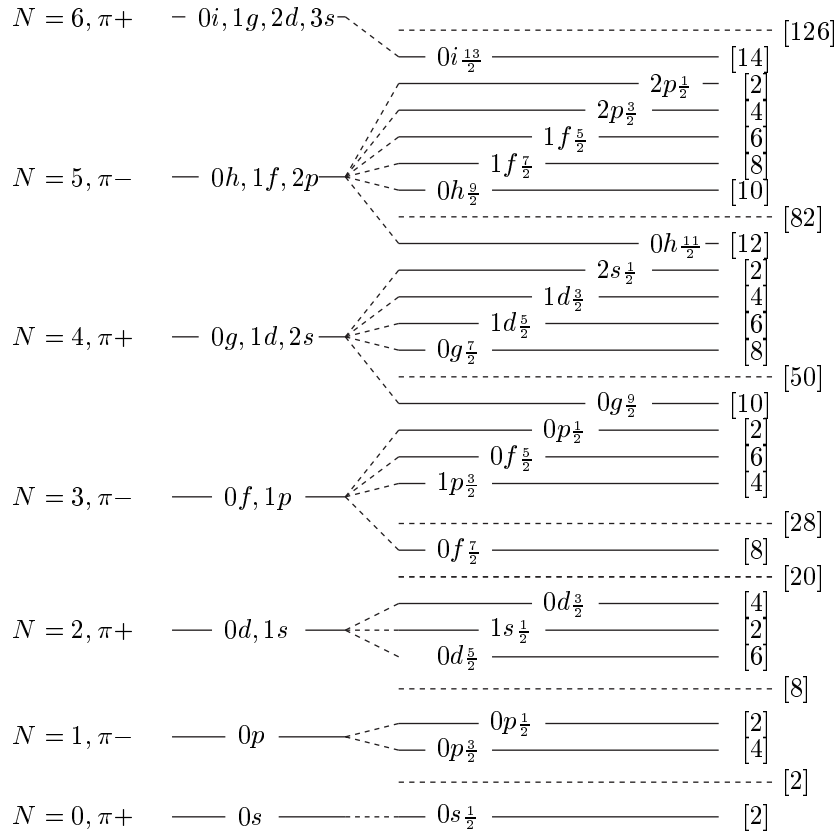


Fig. 3.8 Schematic energy levels for nucleons with inclusion of a substantial spin-orbit potential. Appropriate shell closures are listed in the rightmost column.

The interaction between nucleons is not completely understood theoretically. In principle, one would like to derive the interaction between nucleons from a QCD perspective. This may not occur in the near future, however. Protons and neutrons will remain relevant degrees of freedom to describe nuclei on account of the energy scales involved for nuclear excitations. One therefore proceeds in a practical way and employs experimental data that describe the two-nucleon system to construct interactions that describe these data accurately. Different interactions exist that are able to describe these data equally well but they differ at distances not probed by energies corresponding to elastic nucleon-nucleon (NN) scattering. Some aspects of these interactions are discussed in Ch. 5. This description will thus involve the use of non-relativistic quantum mechanics and the cor-

responding Schrödinger or Lippmann-Schwinger equation. At 140 MeV excitation energy in the two-nucleon system it becomes possible to create an additional pion. These mesonic degrees of freedom are usually not considered explicitly when one is interested in describing nuclear excitations below this threshold. Consequently, one often studies the nuclear many-body problem with a Hamiltonian of the form given by Eq. (2.48) with a two-body interaction V which describes all low-energy two-nucleon data in a nonrelativistic framework. The long-range part of this interaction is accurately described by the exchange of a virtual pion (not enough energy to make it real). In commonly used language, such experimentally constrained interactions are characterized as “realistic”. The nuclear many-body problem is therefore defined but restrictions are obvious: excitations at higher energy than 140 MeV cannot be described realistically. Nevertheless, it will be possible to understand much of the many-particle aspects of the nucleus by considering such a Hamiltonian. This does not need to be too surprising since the coupling to the physical states above 140 MeV is, albeit indirectly, experimentally constrained and the medium modifications of the interaction and the properties of nucleons are most sensitive to an energy scale which is related to shells near the Fermi energy, *i.e.* the energy scale associated with moving nucleons from occupied to empty levels.

3.3.1 *Empirical Mass Formula and Nuclear Matter*

Important qualitative aspects of nuclei that require an explanation from many-body theory are revealed by the systematics of nuclear binding as a function of N and Z and the experimental observation that the density in the interior of nuclei is constant. The systematics of nuclear binding is shown in Fig. 3.9 where the binding energy (Eq. (3.34)) per nucleon is plotted as a function of $A = N + Z$. For each value of A the most stable nucleus was used for the experimental point. A smooth curve through these experimental data is obtained by means of the following expression which is referred to as the semi-empirical mass formula

$$B = b_{vol}A - b_{surf}A^{2/3} - \frac{1}{2}b_{sym}\frac{(N - Z)^2}{A} - \frac{3}{5}\frac{Z^2e^2}{R_c}. \quad (3.33)$$

A relevant set of values of the parameters is given by: $b_{vol} = 15.56$ MeV, $b_{surf} = 17.23$ MeV, $b_{sym} = 46.57$ MeV, and $R_c = 1.24A^{1/3}$ fm. Most nuclei have a binding energy of about 8 MeV per particle which is rather small compared to the rest mass of the nucleon which is about 939 MeV. A plot

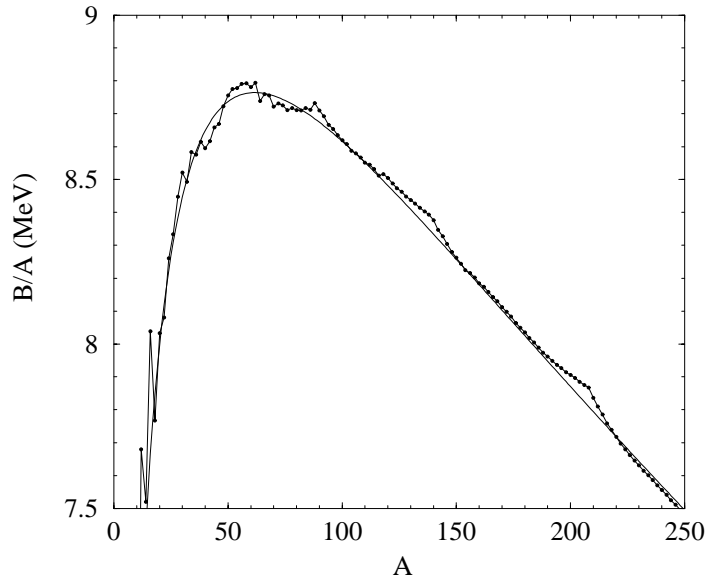


Fig. 3.9 Binding energy per nucleon according to the empirical mass formula given in Eq. (3.33) compared with the experimental binding for the most stable nucleus at a given A as a function of A .

of the binding energy per nucleon as a function of A according to Eq. (3.33) (evaluated for a given A at the most stable value of N) is compared with the corresponding experimental data in Fig. 3.9. The term proportional to the number of particles in the mass formula is called the volume term. The second term represents the loss of attraction due to the presence of the surface and reflects the lack of neighbors to interact in this region. These first two terms suggest a saturation of the nuclear interaction, implying that nucleons on the average experience attraction from interacting with other nucleons only at rather short-range. The third term incorporates the tendency of the nuclear force to favor nuclei with $N = Z$ and is called the symmetry energy. The last term represents the energy of a uniformly charged sphere of radius R_c .

In the case one could switch off the Coulomb interaction between the protons only the volume term survives for $N = Z$ in the limit of infinite volume and constant density. This limit is extremely relevant since, as already mentioned, the central density in the interior of nuclei is found to be constant. From sophisticated elastic electron scattering experiments one de-

duces the charge density at the center of a nucleus; multiplying this number with A/Z one obtains the aforementioned constant central density of 0.16 nucleons per fm^3 . This hypothetical system is referred to as “nuclear matter”. The properties of this system characterize essential global properties of nuclei. The explanation of the saturation density of nuclear matter and the corresponding binding energy per particle of about 16 MeV, starting from a realistic two-body interaction, indeed is a problem in many-particle physics which continues to be studied to this day. The goal of studying this nuclear matter problem is then to explain why a minimum in the energy per particle of -16 MeV occurs at a density of 0.16 fm^3 . In addition, one must quantitatively reproduce these numbers applying many-particle methods. A typical failure until recently has been that when the correct energy at saturation was obtained, this saturation density is about a factor of two too high, or when the correct saturation density was obtained, the energy is only about half of what is required.

3.4 Second quantization and isospin

Neutrons and protons display the same magic numbers and therefore follow the same shell structure. This cannot be an accident. In effect, the mass difference of the neutron and the proton is only about one part in a thousandth of the average of the proton and neutron mass. According to quantum mechanics, this degeneracy must reflect a symmetry of the Hamiltonian describing the strong interaction. In other words, there is an observable which commutes with the Hamiltonian H_S that governs the strong interaction. As a consequence, simultaneous eigenstates of this observable and H_S can be found. Assuming then that the strong force is independent of particle type, one can further neglect the weak and electromagnetic interaction which do distinguish between the proton and the neutron, and eliminate the small mass difference.

In the following discussion [Georgi (1982)] an explicit distinction is made between particle addition and removal operators for protons and neutrons. For example the operator p_α^\dagger adds a proton with quantum numbers α to any state in Fock space and the operator n_α^\dagger does the same for a neutron. These operators obey the same anticommutation relations that were studied before

$$\{p_\alpha^\dagger, p_\beta\} = \delta_{\alpha,\beta}$$

$$\{n_\alpha^\dagger, n_\beta\} = \delta_{\alpha,\beta} \quad (3.34)$$

with all other anticommutators equal to zero including those involving proton and neutron operators. A Z proton state in this notation is then given by

$$|\alpha_1\alpha_2\dots\alpha_Z\rangle = p_{\alpha_1}^\dagger p_{\alpha_2}^\dagger \dots p_{\alpha_Z}^\dagger |0\rangle, \quad (3.35)$$

and a state with N neutrons by

$$|\beta_1\beta_2\dots\beta_N\rangle = n_{\beta_1}^\dagger n_{\beta_2}^\dagger \dots n_{\beta_N}^\dagger |0\rangle. \quad (3.36)$$

A state with Z protons and N neutrons is then given by

$$|\alpha_1\alpha_2\dots\alpha_Z; \beta_1\beta_2\dots\beta_N\rangle = p_{\alpha_1}^\dagger p_{\alpha_2}^\dagger \dots p_{\alpha_Z}^\dagger n_{\beta_1}^\dagger n_{\beta_2}^\dagger \dots n_{\beta_N}^\dagger |0\rangle \quad (3.37)$$

Observing that at the sp level the interchange of a proton for a neutron with otherwise identical quantum numbers does not change the energy, one can postulate that this should be valid also for any collection of protons and neutrons. The corresponding operators are easily written down in second quantization. The operator which changes neutrons into protons, while leaving all other quantum numbers unchanged, is given by

$$\hat{T}^+ = \sum_\alpha p_\alpha^\dagger n_\alpha \quad (3.38)$$

and

$$\hat{T}^- = \sum_\alpha n_\alpha^\dagger p_\alpha \quad (3.39)$$

does the opposite. The assumption is now, based on the degeneracy of the neutron and proton energy, that

$$[\hat{H}_S, \hat{T}^\pm] = 0. \quad (3.40)$$

Consider now the following commutator of \hat{T}^+ and \hat{T}^- denoted by \hat{T}_3

$$\begin{aligned} \hat{T}_3 &= \frac{1}{2}[\hat{T}^+, \hat{T}^-] = \frac{1}{2} \sum_{\alpha\beta} (p_\alpha^\dagger n_\alpha n_\beta^\dagger p_\beta - n_\beta^\dagger p_\beta p_\alpha^\dagger n_\alpha) \\ &= \frac{1}{2} \sum_{\alpha\beta} (p_\alpha^\dagger p_\beta \delta_{\alpha,\beta} - n_\beta^\dagger n_\alpha \delta_{\alpha,\beta}) = \frac{1}{2} \sum_\alpha (p_\alpha^\dagger p_\alpha - n_\alpha^\dagger n_\alpha). \end{aligned} \quad (3.41)$$

This operator merely counts the number of protons and subtracts the number of neutrons (multiplied by 1/2) and physically one expects

$$[\hat{H}_S, \hat{T}_3] = 0. \quad (3.42)$$

One can also show that

$$[\hat{T}_3, \hat{T}^\pm] = \pm \hat{T}^\pm. \quad (3.43)$$

This implies that these operators satisfy the same algebra as the angular momentum operators. Indeed, defining

$$\hat{T}_1 = \frac{1}{2}(\hat{T}^+ + \hat{T}^-) \quad (3.44)$$

and

$$\hat{T}_2 = \frac{1}{2i}(\hat{T}^+ - \hat{T}^-), \quad (3.45)$$

there is a one-to-one correspondence between the triplet (T_1, T_2, T_3) and the triplet of angular momentum operators (J_x, J_y, J_z) including identical commutation relations. Since the spectrum of the angular momentum operators \mathbf{J}^2 and J_z is solely determined by the commutation relations between J_x, J_y , and J_z , one can simply relabel all these results in terms of new quantum numbers related to the operators \mathbf{T}^2 and T_3 which are referred to as total isospin (squared) and its 3-projection. The isospin invariance of the strong interaction therefore means that the strong Hamiltonian is invariant under isospin rotations which are generated by the operators T_1, T_2 , and T_3 in complete analogy with the angular momentum case. Rotations in “iso”-space can therefore be written as

$$R(\hat{n}) = \exp\{-i\hat{n} \cdot \mathbf{T}\}. \quad (3.46)$$

Physical states can be labeled with isospin quantum numbers T and M_T , for total isospin and its third component, respectively. Although only states with T_3 as a good quantum number are observed, one can use the full apparatus of angular momentum algebra in making use of the isospin symmetry of the strong interaction. Clebsch-Gordan coefficients can be used for example to couple states to good total isospin. In the example of the proton-neutron doublet one has total isospin $t = \frac{1}{2}$ and one arbitrarily assigns the proton isospin 3-projection $m_t = \frac{1}{2}$ and the neutron $m_t = -\frac{1}{2}$. Historically, this was done the other way around in nuclear physics in order to make T_3 positive for nuclei with neutron excess, which represent the vast majority of stable nuclides.

Instead of dealing separately with neutrons and protons one can now use the isospin formalism. The complete set of nucleon quantum numbers must then include isospin. For example, a proton at \mathbf{r} with spin projection m_s is denoted by

$$|\mathbf{r}m_s\rangle_p = |\mathbf{r}m_s m_t = \frac{1}{2}\rangle, \quad (3.47)$$

where the total isospin quantum number $t = \frac{1}{2}$ has been suppressed just like the spin $s = \frac{1}{2}$ quantum number. For a neutron one has similarly

$$|\mathbf{r}m_s\rangle_n = |\mathbf{r}m_s m_t = -\frac{1}{2}\rangle. \quad (3.48)$$

One also has

$$\mathbf{T}^2 |\mathbf{r}m_s m_t\rangle = \frac{1}{2}(\frac{1}{2} + 1) |\mathbf{r}m_s m_t\rangle \quad (3.49)$$

and

$$T_3 |\mathbf{r}m_s m_t\rangle = m_t |\mathbf{r}m_s m_t\rangle. \quad (3.50)$$

Note that we are actually thinking of particles in an isospin multiplet as identical particles with T_3 as just another label for the state. For this reason the choice was made to let the proton addition and removal operators anticommute with those for neutrons. Examples of the application and usefulness of the isospin concept abound in nuclear physics.

Before considering the determination of the isospin of a closed-shell, it is useful to present the similar case of the angular momentum of such a system. In order to determine the angular momentum of a closed shell (for example of protons) consider the third component of the total angular momentum operator in second quantization

$$\begin{aligned} \hat{J}_z &= \sum_{n\ell jm} \sum_{n'\ell'j'm'} \langle n\ell jm | j_z | n'\ell'j'm' \rangle a_{n\ell jm}^\dagger a_{n'\ell'j'm'} \\ &= \sum_{n\ell jm} \hbar m a_{n\ell jm}^\dagger a_{n\ell jm}. \end{aligned} \quad (3.51)$$

Without loss of generality one can let this operator act on one full shell where all the particles have quantum numbers n, ℓ, j and all components of j_z are occupied

$$\begin{aligned} \hat{J}_z |n\ell j; m = -j, -j + 1, \dots, j\rangle &= \\ \sum_m \hbar m a_{n\ell jm}^\dagger a_{n\ell jm} |n\ell j; m = -j, -j + 1, \dots, j\rangle \end{aligned}$$

$$\begin{aligned}
&= \left\{ \sum_{m=-j}^j \hbar m \right\} |n\ell j; m = -j, -j+1, \dots, j\rangle \\
&= 0 \times |n\ell j; m = -j, -j+1, \dots, j\rangle.
\end{aligned} \tag{3.52}$$

This result shows that the z -component of the total angular momentum vanishes. By applying the raising and lowering operator to the closed shell in a similar way, one also obtains a vanishing result which demonstrates that the total angular momentum of this state is zero. This analysis also holds for the total isospin. Note that in that case, for a given shell, both proton and neutron states must be completely filled to yield a total isospin of zero. Similar considerations apply to the closed shells in atoms where the total orbital and spin angular momentum are zero neglecting spin-orbit coupling.

3.5 Exercises

- (1) Consider the magnetic moment of Z electrons in an atom with nuclear charge Z

$$\boldsymbol{\mu} = -\frac{|e|\hbar}{2mc} \sum_{i=1}^Z (\boldsymbol{\ell}_i + 2\boldsymbol{s}_i).$$

- a) Determine the second quantized form of the z -component of this operator using the single-particle basis which corresponds to the eigenstates of the single-particle Hamiltonian which treats the other electrons in central-field approximation (see Eq. (3.13)). Be sure to evaluate the relevant single-particle matrix elements in this basis.
- b) Consider an atom with one electron outside a set of closed shells, occupying the lowest sp state that is not filled. Denote the quantum numbers of this state by n, ℓ, m_ℓ, m_s . Assume that for this last electron $m_\ell = \ell$ and $m_s = 1/2$. Determine the magnetic moment of this atomic state (with one electron outside the closed shells) by calculating the expectation value of the operator obtained in part a) with respect to this state (this is the actual definition of the magnetic moment in this case). When evaluating the magnetic moment, you should carefully consider all possible contributions to this magnetic moment including the one from the closed shells

(if there is any). Compare your result with experimental data for alkali atoms.

- (2) Calculate the magnetic moment of the nuclei ^{15}O , ^{15}N , ^{17}O , and ^{17}F in the independent-particle approximation. The magnetic moment is defined by

$$\mu = \langle JM_J = J | \mu_z | JM_J = J \rangle, \quad (3.53)$$

where for A nucleons the magnetic moment operator (in first quantization) is given by

$$\mu^A = \sum_{i=1}^A \{g_\ell(i)\ell_i + g_s(i)s_i\}. \quad (3.54)$$

The orbital angular momentum factor g_ℓ is 1 in units of nuclear magnetons for protons and 0 for neutrons. The notation above assumes that the orbital and spin angular momentum are in units of \hbar . A nuclear magneton is given by $e\hbar/2m_p c$. In the same units the spin factor g_s is 5.58 for protons and -3.82 for neutrons. Assume that the nuclei listed above correspond to either a missing $p_{1/2}$ proton or neutron in the double closed-shell ^{16}O or a $d_{5/2}$ proton or neutron added to it. Employ the second-quantized operator for the magnetic moment. You then also need to calculate the magnetic moment sp matrix elements. To do this, you could use the projection theorem (see Eq. (3.10.40) in [Sakurai (1994)]). In addition, you will need an argument to demonstrate that closed shells don't contribute. Express your final results in nuclear magnetons and compare with experiment.

- (3) Write down the charge density operator for the nucleus in first quantization but include isospin. Construct the corresponding second-quantized operator. Show that this operator may be written as

$$\hat{\rho}_C(r) = \frac{1}{4\pi} e \sum_{\ell j m_j m_t} (\frac{1}{2} + m_t) a_{r\ell j m_j m_t}^\dagger a_{r\ell j m_j m_t}$$

in the appropriate basis $\{|r(l s) j m_j m_t\rangle\}$. Note that operator is appropriate for a closed-shell system which has no angular momentum. In that case the nuclear charge distribution depends only on r . One may therefore divide the charge density operator by 4π and integrate over all angles to obtain the above expression. Evaluate the expectation value of this operator for the ground state of a doubly closed-shell nucleus.

- (4) Use the Hydrogen-like Hamiltonian for the He atom to approximate the ground state in the independent-particle model. Calculate the energy of the ground state with the inclusion of the expectation values of the two-body electron-electron interaction (first-order perturbation theory) and compare with experiment.